Researchers Journal of Science and Technology (REJOST)

https://rejost.com.ng

Application of Combined 2-Dimensional Imaging and Dipole-Dipole Technique in Depth to Bedrock Delineation within UNIOSUN Main Campus Car Park, Osogbo, Nigeria

[1]Ojo Adeolu Olabanji, [1]Akinyele Olu. Folasade, [1]Oladimeji Gboyega Razaq, [1]Awobode O. Sekinat, [2]Babafemi Emmanuel Olumuyiwa

Received: August 17, 2023 /Accepted: October 6, 2023

Abstract

An integrated geophysical investigation consisting of two-dimensional Wenner resistivity imaging and dipole-dipole techniques was carried out within Osun State University Main Campus, Osogbo, Nigeria on a site temporarily used as public car park. The aim of the study was to image the subsurface conditions of the site and delineates the overburden - bedrock interface of the subsurface in the car park in readiness for the concrete flooring of the car pack and to compare the results from using two different equipment; PASI and integrated geophysical information system (IGIS) terrameters. The Wenner data was interpreted using the MS Excel while the dipole-dipole data was interpreted using DiprofWin software. Interpretation of field data produces 2D Wenner imaging and dipole-dipole pseudo-sections. Dipole-dipole pseudo-section revealed that the subsurface layers of the site comprises of about 10 meters of weak and incompetent sandy layer having a resistivity of 296 Ωm with the layer underlain by a 4-meters thick low-resistance lateritic layer of resistivity value of 372.18 Ωm. The bedrock underlying the sequence is about 15 m deep, with resistivity value between 4169.09 Ωm, and 4670.132 Ωm. The 2-D imaging interpretations using the two pieces of equipment correlate at shallow depth but differ at greater depth. The results obtained from the Wenner interpretation of the two pieces of equipment do

✉ Ojo Adeolu Olabanji: adeolu.ojo@uniosun.edu.ng

[1]Department of Geological Sciences, Osun State University, Osogbo

[2]Geobabs Integrated Services, Lagos, Nigeria

not correlate due to the very high exaggerated values obtained while using the IGIS instrument.

The result concludes that the depth-to-bedrock interface is best defined using the PASI resistivity instrument compared to the IGIS resistivity meter.

Keyword: Osogbo; Resistivity; Overburden; Bedrock; PASI; IGIS.

Introduction

Proper geophysical studies and investigation are very important procedures that are needed to be taken into consideration when carrying out major construction studies. This is because the integrity and durability of any superstructure constructed on any piece of land depend on the foundation architecture of the given area.

Depth-to-bedrock is the total overburden thickness resting on the bedrock (Ibitoye, 2023) or simply the thickness of unconsolidated materials overlying bedrock (Hart *et al.,* 2021). Depth-to-bedrock determination is of great importance because it provides the link between the underlying geology in any place, groundwater movement, as well as the land use. Hence they are useful in guiding many activities, such as installation of utilities, permitting, and construction of bridges, walkways, pavements and concrete parks, wind farms and the land application of waste products in sensitive areas where depth-to-bedrock is restricted (Hart *et al.*, 2021).Geologic bedrock under any superstructure could be sedimentary, igneous, or metamorphic origin. The weathering of these basement rocks produces the overburden. Overburden and basement rocks have different properties. In terms of density, bedrock has higher density than the overburden and in terms of resistivity; bedrock is more resistive than the overburden. The knowledge of the depth-to-bedrock/overburden interface is essential to a geoscientist, especially during engineering investigations, mineral exploration, construction workers, etc. This is because it gives an idea about the depth of the competent layer (to an engineer) and the depth of target deposit (to a geoscientist). The only way to delineate the interface between the two is by collecting core cuttings (i.e., samples) during drilling of the subsurface. Drilling helps to bring out core samples from the subsurface and determine the depth of bedrock. The determination of the interface between bedrock and the overburden usually ends up disturbing and destroying the subsurface layers. Sometimes, it could involve core logging at intervals and description as drilling progresses-an exercise that could be arduous and tasking. Also, quite a number of drill core samples are needed to be collected and described in order to achieve the objectives. Hence, there is a need to look elsewhere to find an alternative means.

Geophysical methods have proved to be of great usefulness, especially in the recognition of subsurface structures by observing anomalies in their geophysical properties. It represents an effective way of recognizing and delineating the subsurface discontinuities that camouflage as anomalies. These include voids, groundwater, bedrock, and the likes (Mochales *et al.*, 2008).Seismic refraction, ground penetrating radar and electrical methods have been extensively utilized since they possess the ability to reveal better images of subsurface inhomogeneous attributes(Hirsch *et al*., 2008; Tye *et al*., 2011). Combined electrical resistivity tomography and induced polarization techniques have also been employed in mineral exploration, especially in characterization and mapping of (Pb-Zn-Ag) sulfide deposits (Ali et al., 2023). Zhou, (2000) also have been able to show that of all techniques of electrical resistivity methods in geophysical prospecting, the dipole-dipole

electrical resistivity tomography have been very effective and reliable in defining depth-to-bedrock especially in covered karst terranes. Briggs *et al.*, (2022) were able to investigate how local bedrock depth control summer stream temperature and channel disconnection (dewatering), by measuring stream corridor bedrock depth using horizontal-to-vertical spectral ratio (HVSR) approach - a passive seismic technique which uses the principle of evaluating ambient seismic noise recorded using handheld seismic tool placed on the ground surface to identify seismic resonance generated due to strong vertical changes in subsurface acoustic impedance.

Seismic refraction and ground penetrating radar (GPR) surveys make use of expensive equipment and usually involve high manpower (especially seismic refraction). On the other hand, electrical resistivity tools are cheaper, less laborious and require less manpower. As a result, it has become a useful and versatile method employed by most geoscientists and also gives the results compared to other geophysical methods. For instance, electrical resistivity tomography (ERT), a type of electrical resistivity technique, has been proven to be an effective means of studying the bedrock architecture (Froese *et al*., 2005; Hickin *et al*., 2009; Hsu *et al.*, 2010), mapping geological structures (Tye*et al.*, 2011), delineation of subsurface groundwater-bearing intervals (Hirsch *et al.*, 2008; Revil *et al.*, 2005) and also in mineral exploration activities.

Workers such as Salami and Babafemi (2020) have employed the use of 1-D and 2-D subsurface resistivity imaging to delineate near-surface structural features in Igarra, Akoko-Edo, South and western Nigeria. They observed that the northeastern part of the survey area possesses a high possibility of fracturing within the underlying basement. The work also revealed the main lithologies constituting the materials that form the overburden to be sandy clay, lateritic sand and weathered basement. Other workers include Neyamadpour *et al.* (2010) who carried out near-surface electrical resistivity imaging around the University of Malaya, Malaysia using2D and 3DWenner and the dipole-dipole technique. The results of dipole–dipole and Wenner array survey techniques in the delineation of a subsurface three-dimensional cavity were compared. The work established the superiority of the Wenner array over the dipole - dipole array in detecting vertical variation of subsurface resistivity. However, the dipole - dipole array result was better than that of the Wenner array in providing a lateral variation of the subsurface resistivities. Panthi *et al.* (2020) also attempted the delineation of the bedrock topography using the electrical resistivity technique and ended up producing a high resolution topography map of bedrock with depth of about 80m. Two electrical resistivity tomography profiles were used to cross-validate the results by carrying out one inland and the other in a seaside environment. The results showed good agreement with the subsurface layer contrast in resistivity. This indicates that the technique supplements, in a way, the resistivity data interpretation in subsurface mapping of structures and features. Najafabadipour and Kamali (2017) also conducted a three-dimensional modeling and bedrock determination survey using electrical resistivity inversion in Estahban city, located in the Fars province of Iran.

In this study, the electrical method is used to map the bedrock/overburden interface within Osun State University around the temporary Korope car park. This was carried out by combining the two-dimensional Wenner imaging and dipole-dipole techniques. Two pieces of resistivity equipment were used in this work: the PASI and

IGIS resistivity machines. This work is of great significance because the management of the university is proposing to erect a befitting and well-grounded well floored car park that will support all kinds of vehicles on this site. This can only be achieved by investigating of the subsurface of the site and detecting any geologic, geo-technique and structural parameters that could undermine the siting of the superstructure. The electrical resistivity survey will assist in the determination of the subsurface resistivity distribution, the car park foundation investigation, as well as the depth of the competent layer within the car park. Dipole-dipole and Wenner array techniques of electrical resistivity methods are two important horizontal profiling techniques of electrical resistivity methods that find great application and reasonable results when it comes to revealing the shallow vertical variation in the sub-surface resistivity as well as the lateral variation in the resistivity as well.

Location of the Study Area

The study area under investigation is located within the main campus of Osun State University, Osogbo. The university is located in Osogbo, the Osun State capital and administrative headquarters of Osogbo Local Government, in the Southwestern part of Nigeria. It is situated along Ibokun Road in the Shasha area of Oke-Baale. The site of investigation is located at Korope Car Park within the Latitudes of 07^{o} 45' 42.78'' N - 07^{o} 45' 43.74'' N and 04^{o} 36' 11.68'' E - 04^{o} 36' 10.68'' E. The study area is generally accessible from Ibokun Road via the University Road that links the main road to the university.

Generally, Osogbo and its environs are drained by the famous River Osun, which divides into smaller distributaries and streams but ends up drying up especially between November and April. The drainage pattern of the study area is mostly dendritic; hence are controlled most of the times by the structures and local geology of the study area. The study area possesses moderate to low relief and is situated about 341m above sea level. The study area slopes gently from the main gate towards the school and begins to rise gently at the Health Centre towards the Administrative building, creating a little depression with a stream (around the Health Centre) inside which water flows during high rain fall towards the eastern part. The study area falls within a low land tropical rainforest with little vegetation. Multiple canopies and lianas dominate this area, but most of them have been giving way to secondary forest and derived savannah as a result of continuous cultivation and bush burning for years. The only reserved forest within Osogbo metropolis is the one inside the Osun Osogbo groove. The environmental air temperature is high in most parts of the year and the temperature rangesbetween27°C and 33°C, with the maximum temperature occurring around April (United Nations Human Settlements Program, 2014). The dry season extend from January to April, while the wet season lasts from June to October, with an average temperature of 33^{o}C on a daily basis. March happens to be the hottest month of the year in Osogbo and it has an average high temperature of about 33°C while 27°C is the average low temperature. August every year is the coldest month of the year and it has an average lowest temperature of 24°C while 27°C is the highest temperature.

The study area is located in the upper part of the tropical hinterland climatic region, has a humid tropical climate. It has a distinct wet and dry season (United Nations Human Settlements Program, 2014). The wet season commences in March and ends in October. However, due to variations in climate characteristics in recent times, it has extended into the first and second weeks of November. Rainfall occurs in these

eight months of the year. Annual rainfall fall between1200 and 1500 mm per year and they peak in September. Cyclonic rainfall is very common in Osogbo and does come with double maxima around June/July as well as September/October. When the intensity of solar radiation and humidity conditions are high, conventional rainfall is experienced. The relative humidity is about 80% averagely every year.

Geologically, Osogbo and its environs constitute part of the Basement Complex zone of Southwestern Nigeria. This zone consists of migmatite-gnesis, quartzite, quartz schist zone and it lies within the zone of Pan African reactivation of 600±150m.y (Olabanji, 2016).A large proportion of the top soil in most cases comprises of lateritic soils or laterite, which are usually derived from the weathering of underlying parent metamorphic rocks (migmatites, schist, gneisses) or igneous rocks (basalts, peridotite, granites and gabbros). The major lithology of the study area is schist and banded-gneiss

.

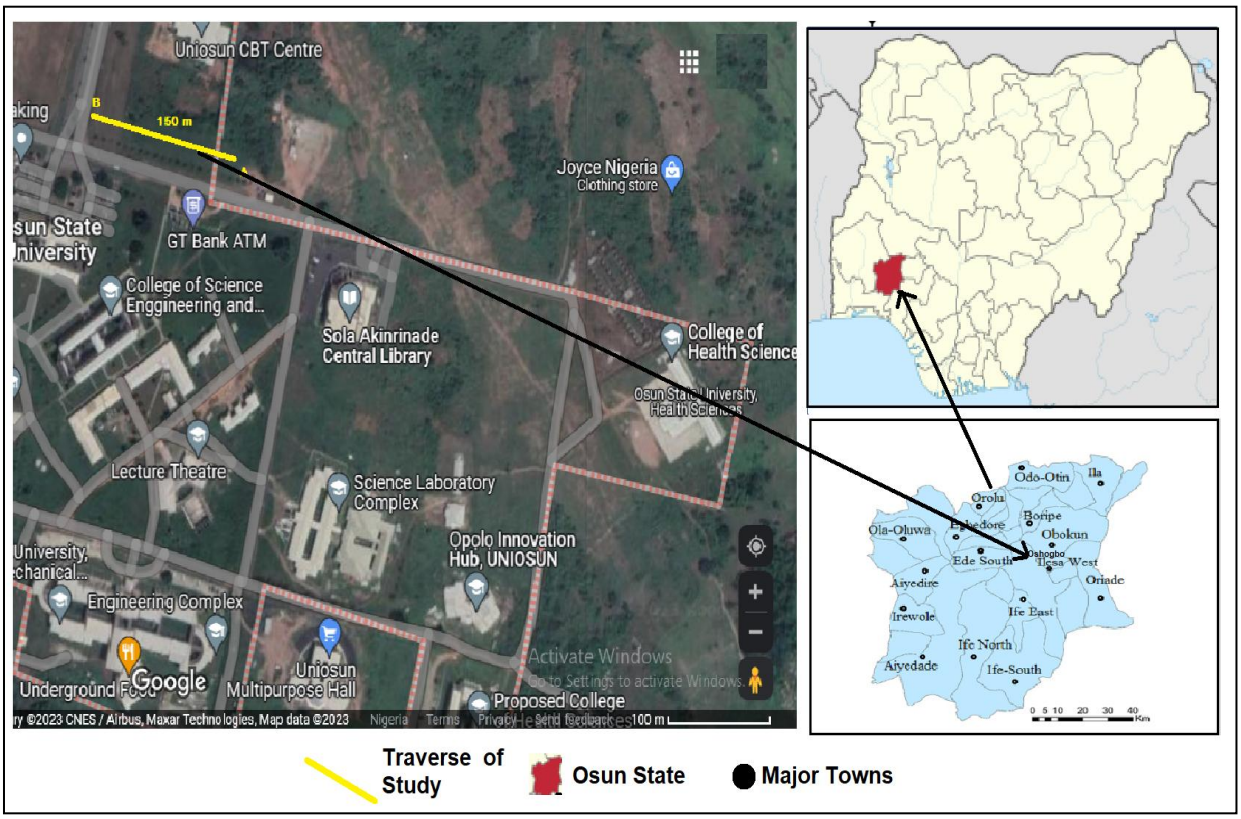

Figure 1: Aerial Map of the study area showing the position of the traverse.

Materials and Methods

This project was conducted in stages. The first stage was preliminary reconnaissance survey of the site in order to investigate the lateral extent of the car park and the selection of places where possible traverse could be established. The two pieces of resistivity equipment were used for the investigation with the intention of comparing result of the imaging obtained using the two equipment – the Integrated Geophysical

Information System (IGIS) and PASI resistivity meters. A 150m traverse was first established, along which the investigation was carried out. The Wenner survey was first conducted with an electrode spacing interval of 10 m and the current (C1 and C2) electrodes were spaced out, while the potential electrodes (P1 and P2) were also spaced out accordingly with the first and last points along the traverse properly georeferenced. Interpretation of the dipole-dipole data field was done and inverted using the DiprofWin software, while the 2-D Wenner data was interpreted using the Microsoft Excel package.

Presentation and Discussion of Results

Tables 1 and 2 represent the data obtained using the dipole-dipole array technique by PASI and IGIS resistivity meter respectively while Table 3 and 4 are the 2-D Wenner survey data collected using IGIS resistivity meter and PASI resistivity meter respectively. The pseudo-section produced from the interpretation of the dipole-dipole data is as shown in Figures 2 and 3 while that produced from the interpretation of the Wenner survey data is as shown in Figures 4 and 5.

Discussion of Results

Dipole-Dipole Interpretation

2-D pseudo-sections were generated from the dipole-dipole data collected from the traverses. The exercise was carried out with respect to the elevation of the site above sea level (in meters). This is as shown on the left and right flanks of the 2-D pseudo-sections. It was also carried out in order to correlate the result obtained with 2D Wenner data-generated geo-electric pseudo-sections. Also on display in the 2-D resistivity section is the vertical and lateral change in resistivity along the profile. The elevation of the site is about 341m with a survey depth of about 50m. In order to ease the interpretation procedure, colour bands within the range and shades of purple/deep red to shades of green and deep blue were employed; the extreme of purple/deep red signifying a highly resistive interval, while shades of green to deep blue signify weak zones with lower resistivity.

The values of the resistance measured during the use of the PASI to acquire dipole-dipole data varied along the traverse from as low as 0.748 Ω close to the middle of the traverse and at shallow depth to as high as 39.7 Ω at the earlier portion of the traverse and at greater depth. Hence, the resistivity values obtained varied from as low as 70.497 Ωm at shallow depth to as high as 74832.27532 Ωm at greater depth (see Table 1). The dipole-dipole of the PASI data is as shown in Figure 2. Here, from the figure, it is evident that the resistivity increases with depth, with low resistivity materials at the top while high resistive and competent materials at depth. Interpretation revealed a near-surface low resistivity value at shallow depth of about 10m (blue and green), which represents the incompetent sandy material on the interpreted inverted 2-D pseudo-section. This varies in resistivity from 296 to 3322Ωm. The basement zone extends from around 12 m to 50 m depth along the 2D resistivity pseudo-section, with very high resistivity values showing a competent layer of bedrock.

Table 2 represents the variation in the resistance and hence resistivity of the subsurface horizontally and vertically along the traverse using the IGIS machine to acquire the dipole-dipole technique. Here, the resistance is as low as 3 Ωm close to the middle of the traverse and at shallow depth to as high as 47.2 Ωm at the earlier portion of the traverse. This resulted in the relatively low resistivity at shallow depth, with the shallow depth (blue and green portion, and usually less than or equal to 10 m) having resistivity of s low as 1130.9733 Ωm while the deeper resistivity is as high as 4,448.496165 Ωm at deeper depth. The result of the pseudo-section

is as presented in Figure 3. Although the signature produced from the interpretation of the data collected using the two pieces of equipment seem to correlate, the resistivity values using the IGIS machine are highly exaggerated far above that obtained using PASI equipment. . This inverted two-dimensional resistivity pseudo-section shows similar values for incompetent earth materials near the surface at shallow depth and a very high resistivity competent resistivity layer as the first dipole-dipole.

From the investigation, it is evident that the 2-D imagery obtained from the interpretation of the two data collected using the two pieces of equipment (PASI and IGIS) gave a similar signature at shallow depth but slightly differed in signature at deeper depth.

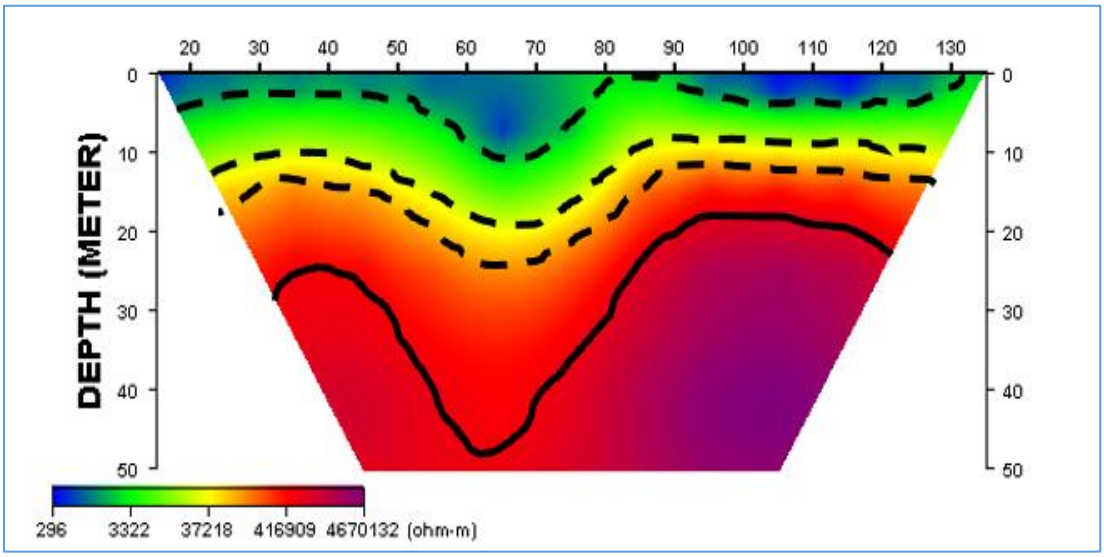

Figure 2: Korope car park Dipole-Dipole (PASI) Pseudo-section

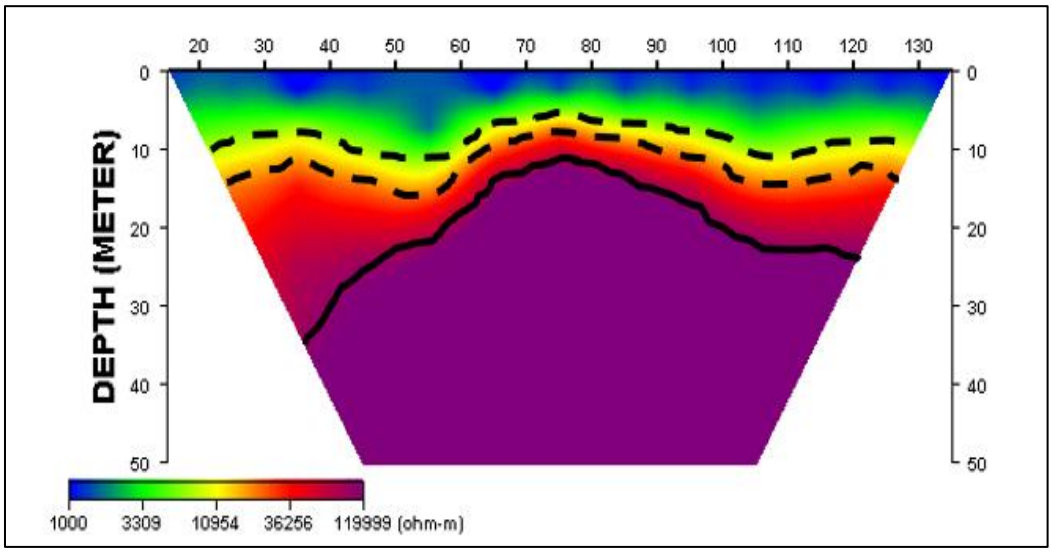

Figure 3: Korope car park Dipole-Dipole (IGIS) Pseudo-section

Table 1: Dipole-Dipole PASI Data Sheet 1

Date: June 22, 2022		**Observer: (Ojo et al. 202 2)**				
Equipment: PASI Resistivity Meter				**Survey: Dipole-Dipole**		
C1	**C2**	**P1**	**P2**	**GEOMETRIC FACTOR (K) (in m)**	**Resistance (Ω)**	**Apparent Resistivity (Ωm)**
0	1	2	3	94.2478	3.6	339.29208
		3	4	376.9911	4.8	1809.55728
		4	5	942.4778	12.2	11498.22916
		5	6	1884.9556	35.2	66350.43712
		6	7	1884.9556	31	58433.6236
1	2	3	4	94.2478	5.5	518.3629
		4	5	376.9911	19.5	7351.32645
		5	6	942.4778	7.1	6691.59238
		6	7	1884.956	39.7	74832.7532
		7	8	3298.672	23.9	78838.2608
2	3	4	5	94.2478	15.4	1451.41612
		5	6	376.9911	8.7	3279.82257
		6	7	942.4778	6.6	6220.35348
		7	8	1884.956	10.4	19603.5424
		8	9	3298.672	5.3	17482.9616
3	4	5	6	94.2478	0.748	70.4973544
		6	7	376.9911	4.3	1621.06173
		7	8	942.4778	19.6	18472.56488
		8	9	1884.956	7.8	14702.6568
		9	10	3298.672	3.7	12205.0864
4	5	6	7	94.2478	6.5	612.6107
		7	8	376.9911	4.3	1621.06173
		8	9	942.4778	6	5654.8668
		9	10	1884.956	21.3	40149.5628
		10	11	3298.672	26.8	88404.4096
5	6	7	8	94.2478	2.9	273.31862
		8	9	376.9911	9.4	3543.71634
		9	10	942.4778	6.4	6031.85792
		10	11	1884.956	27.5	51836.29
		11	12	3298.672	26.8	88404.4096
6	7	8	9	94.2478	11.8	1112.12404
		9	10	376.9911	2.1	791.68131
		10	11	942.4778	9.5	8953.5391
		11	12	1884.956	10.2	19226.5512
		12	13	3298.672	2.2	7257.0784
7	8	9	10	94.2478	21.2	1998.05336

		10	11	376.9911	19.5	7351.32645
		11	12	942.4778	10.4	9801.76912
		12	13	1884.956	8.9	16776.1084
		13	14	3298.672	9.2	30347.7824
8	9	10	11	94.2478	16	1507.9648
		11	12	376.9911	19	7162.8309
		12	13	942.4778	17.4	16399.11372
		13	14	1884.956	22	41469.032
		14	15	3298.672	15.6	51459.2832
9	10	11	12	94.2478	1.9	179.07082
		12	13	376.9911	12.9	4863.18519
		13	14	942.4778	31.2	29405.30736
		14	15	1884.956	11.8	22242.4808
10	11	12	13	94.2478	1.9	179.07082
		13	14	376.9911	8.3	3129.02613
		14	15	942.4778	31.4	29593.80292
11	12	13	14	94.2478	17.4	1639.91172
		14	15	376.9911	26	9801.7686
12	13	14	15	94.2478	3.7	348.71686

Table 2: Dipole-Dipole IGIS Data Sheet 2

Date: June 22, 2022				**Observer: Ojo et al**	
Equipment: IGIS Resistivity Meter				**Survey: Dipole-Dipole**	
C1	**C2**	**P1**	**P2**	**GEOMETRIC FACTOR (K) in (m)**	**Resistance (Ω)**	**Apparent Resistivity (Ωm)**
0	1	2	3	94.2478	45.6	4297.69968
		3	4	376.9911	19.8	7464.42378
		4	5	942.4778	28.2	26577.87396
		5	6	1884.9556	29	54663.724
		6	7	1884.9556	32.7	107866.5744
1	2	3	4	94.2478	5.3	499.51334
		4	5	376.9911	17.5	6597.34425
		5	6	942.4778	4.5	4241.1501
		6	7	1884.956	37	69743.372
		7	8	3298.672	9.3	30677.6496
2	3	4	5	94.2478	47.2	4,448.49616
		5	6	376.9911	7	2638.9377
		6	7	942.4778	3	2827.4334
		7	8	1884.956	5	9424.78
		8	9	3298.672	16	52778.752
3	4	5	6	94.2478	8	753.9824

		6	7	376.9911	3	1130.9733
		7	8	942.4778	4	3769.9112
		8	9	1884.956	7	13194.692
		9	10	3298.672	27.3	90053.7456
4	5	6	7	94.2478	4.75	447.67705
		7	8	376.9911	8	3015.9288
		8	9	942.4778	7.5	7068.5835
		9	10	1884.956	24	45238.944
		10	11	3298.672	2.75	9071.348
5	6	7	8	94.2478	34.75	3275.11105
		8	9	376.9911	9	3392.9199
		9	10	942.4778	23.5	22148.2283
		10	11	1884.956	41.75	78696.913
		11	12	3298.672	2	6597.344
6	7	8	9	94.2478	14	1319.4692
		9	10	376.9911	24	9047.7864
		10	11	942.4778	10	9424.778
		11	12	1884.956	11	20734.516
		12	13	3298.672	10	32986.72
7	8	9	10	94.2478	12.6	1187.52228
		10	11	376.9911	7.3	2752.03503
		11	12	942.4778	4.3	4052.65454
		12	13	1884.956	5.5	10367.258
		13	14	3298.672	11	36285.392
8	9	10	11	94.2478	2.25	212.05755
		11	12	376.9911	5.75	2167.698825
		12	13	942.4778	3.5	3298.6723
		13	14	1884.956	5	9424.78
		14	15	3298.672	13	42882.736
9	10	11	12	94.2478	10.25	966.03995
		12	13	376.9911	16.5	6220.35315
		13	14	942.4778	7.25	6832.96405
		14	15	1884.956	8	15079.648
10	11	12	13	94.2478	23.5	2214.8233
		13	14	376.9911	4	1507.9644
		14	15	942.4778	33	31101.7674
11	12	13	14	94.2478	15	1413.717
		14	15	376.9911	21.5	8105.30865
12	13	14	15	94.2478	3.7	348.71686

Wenner Data Interpretation and Imaging

Tables 3 and 4 represent the Wenner data obtained with the use of the PASI and the IGIS resistivity meters. In Table 3, the apparent resistivity measured by the PASI equipment varied from few hundreds (235.0 to 439.1 Ωm) at earlier portion of the traverse to several hundreds to thousands (754.08 Ωm to 4,524 Ωm) along the traverse. Lithology identified consists of purely lateritic materials of diverse resistivity at shallow depths. Figures 4 and 5 represent the inverted 2D Wenner imaging sections of the resistivity data acquired along the traverse using the two pieces of equipment. This interpretation revealed more information about the subsurface lithological sequence, including the depth of the bedrock. From figure 4, this observation occurred between depths of 10 to 18 meters (Table 3). The geoelectric pseudo-sections generated from 2D Wenner resistivity data displays the vertical and lateral changes in resistivity along a profile. The first 2D Wenner imaging carried out using the PASI resistivity meter possesses a subsurface high-resistivity earth material (represented with red and purple) that ranges in resistivity from about 223 to 500Ωm. It extends between 0 and 25 m covering the entire horizontal extent of the interpreted inverted 2-D pseudo-sections which is generally not normal because the high resistivity represents the basement zone, but in this case, they are found closer to the surface at shallow depth. The basement zone extends from around 25-50 meters depth along the vertical scale 2D resistivity pseudo-sections with very low resistivity values ranging from 100 Ωm to 223 Ωm in colour (blue and green). In these inverted 2-D pseudo-sections, relatively lower resistivity values are encountered below the subsurface at higher depths while high resistivity values are found in the subsurface, which is generally not possible. This abnormal situation is not uncommon with data collected using PASI equipment. This is due to the erratic behavior of the machine when under stress for a length of time. However, the observation is against what is obtained at greater depths. Profiling result showed that low resistivity values are found at intermediate depths between 10 to 30 meters while very low resistivity values occur at greater depth up to 50 meters and beyond. These depths have low resistivity as low as between 100 Ωm and 149.1 Ωm (blue to yellow colour bands). See Figure 4.

The second 2D Wenner imaging profile conducted using the IGIS resistivity meter taken along the same traverse is as shown in Figure 5. In this case, the topmost soil has a subsurface resistivity value of 223Ωm to 500Ωm. This extends between 0 and 25meters deep and covers the entire long period of the interpreted inverted 2-D pseudo-section. This is not expected because the high resistivity represents the basement zone. In this case, the IGIS resistivity machine gave very high resistivity values, which caused the entire inverted 2D imaging to display a very high profile and show competent layer.

Generally, the entire resistivity value recorded using the IGIS in Wenner survey were observed to be far higher than expected. This is due to the fact that IGIS instruments do exaggerate resistivity values. Most of the resistivity values were observed to be higher than 300 Ωm, with a negligible station having values between 81.2221 and 201.088 Ωm. Other resistivity values were higher than 300 Ωm (Table 4). The Wenner results using the two pieces of equipment do not show clearly the overburden – bedrock interface. Rather, it reports that the study area is composed entire of high resistivity materials with no definite overburden – bedrock interface. On the contrary, the dipole-dipole technique does reveal the overburden – bedrock interface.

Table 3: 2D Wenner IGIS Data Sheet 1

Date: 09-11-2022				**TRAVERSE: 3**		
Coordinate: **Longitude: N7^{o} 45' 42.78''**				**LOCATION: Korope Car Park, UNIOSUN.**		
Latitude: E4^{o} 36' 11.68''				**INSTRUMENT USED: PASI**		
Altitude: 341				**2D -Wenner Profiling Array**		
N1						
C1	P1	P2	C2	RESIS. (Ω)	G.F in (m) = 62.48	App Res (Ωm)
0	10	20	30	5	62.48	312.4
10	20	30	40	11	62.48	687.28
20	30	40	50	34.5	62.48	2155.56
30	40	50	60	8.3	62.48	518.584
40	50	60	70	5.6	62.48	349.888
50	60	70	80	6.8	62.48	424.864
60	70	80	90	7.25	62.48	452.98
70	80	90	100	3	62.48	187.44
80	90	100	110	44	62.48	2749.12
90	100	110	120	10	62.48	624.8
100	110	120	130	4	62.48	249.92
110	120	130	140	9.5	62.48	593.56
120	130	140	150	6.5	62.48	406.12
N2						
0	20	40	60	2.4	125.68	301.632
10	30	50	70	4.6	125.68	578.128
20	40	60	80	17.25	125.68	2167.98
30	50	70	90	22.2	125.68	2790.096
40	60	80	100	36	125.68	4524.48
50	70	90	110	3.5	125.68	439.88
60	80	100	120	6	125.68	754.08
70	90	110	130	6.5	125.68	816.92
80	100	120	140	6	125.68	754.08
90	110	130	150	6.5	125.68	816.92
N3						
0	30	60	90	1.25	188.52	235.65
10	40	70	100	20	188.52	3770.4
20	50	80	110	2	188.52	377.04
30	60	90	120	4	188.52	754.08
40	70	100	130	6	188.52	1131.12
50	80	110	140	42.3	188.52	7974.396
60	90	120	150	23.8	188.52	4486.776
N4						

0	40	80	120	1.6	251.36	402.176
10	50	90	130	1.5	251.36	377.04
20	60	100	140	3	251.36	754.08
30	70	110	150	4	251.36	1005.44
N5						
0	50	100	150	11	314.2	3456.2

Table 4: 2D Wenner PASI Data Sheet 2

Date: 09-11-2022				**TRAVERSE: 4**		
Coordinate: **Longitude: N7^{o} 45' 42.78''**				**LOCATION: Korope Car Park, UNIOSUN.**		
Latitude: E4^{o} 36' 11.68''				**INSTRUMENT USED: IGIS**		
Altitude: 341				**2D -Wenner Profiling Array**		
N1						
C1	P1	P2	C2	RESIS. (Ω)	G.F in (m) = 62.48	App Res (Ωm)
0	10	20	30	37	62.48	2311.76
10	20	30	40	1.3	62.48	81.224
20	30	40	50	33.7	62.48	2105.576
30	40	50	60	53.5	62.48	3342.68
40	50	60	70	40.3	62.48	2517.944
50	60	70	80	46.9	62.48	2930.312
60	70	80	90	31.5	62.48	1968.12
70	80	90	100	51.7	62.48	3230.216
80	90	100	110	39.9	62.48	2492.952
90	100	110	120	18.5	62.48	1155.88
100	110	120	130	15.3	62.48	955.944
110	120	130	140	6.6	62.48	412.368
120	130	140	150	19.6	62.48	1224.608
N2						
0	20	40	60	5.7	125.68	716.376
10	30	50	70	3	125.68	377.04
20	40	60	80	4.1	125.68	515.288
30	50	70	90	3.9	125.68	490.152
40	60	80	100	6.1	125.68	766.648
50	70	90	110	3.8	125.68	477.584
60	80	100	120	4.2	125.68	527.856
70	90	110	130	1.5	125.68	188.52
80	100	120	140	3.7	125.68	465.016
90	110	130	150	1.6	125.68	201.088
N3						

0	30	60	90	9.4	188.52	1772.088
10	40	70	100	1.7	188.52	320.484
20	50	80	110	1.2	188.52	226.224
30	60	90	120	1.6	188.52	301.632
40	70	100	130	0.963	188.52	181.54476
50	80	110	140	0.688	188.52	129.70176
60	90	120	150	4.9	188.52	923.748
N4						
0	40	80	120	14	251.36	3519.04
10	50	90	130	12.3	251.36	3091.728
20	60	100	140	1.9	251.36	477.584
30	70	110	150	3.4	251.36	854.624
N5						
0	50	100	150	32.6	314.2	10242.92

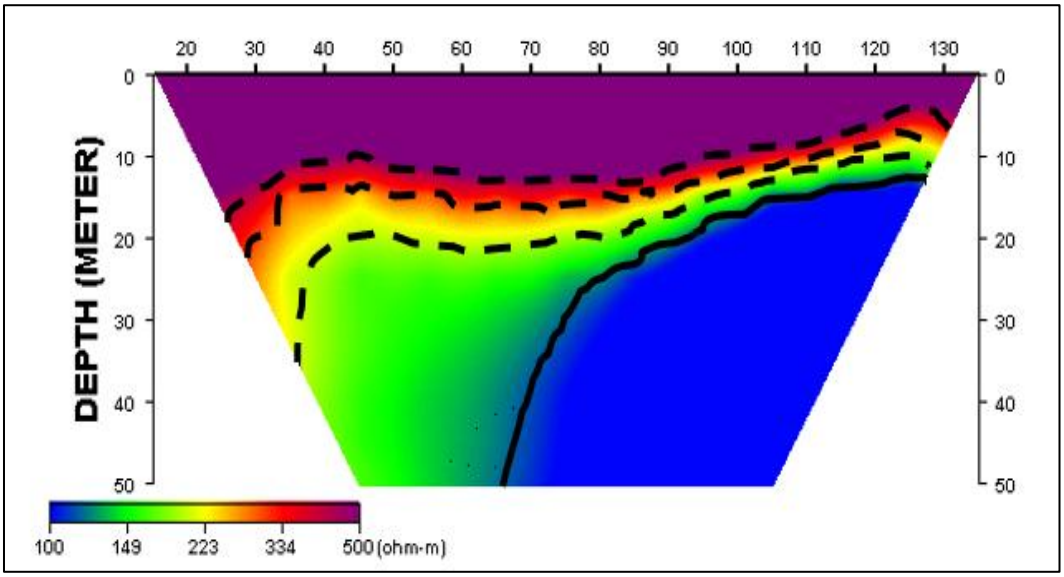

Figure 4: Korope car park 2D-Wenner (PASI) Pseudo-sections

Conclusion

In this project, an integrated geophysical investigation consisting of 2-dimensional Wenner resistivity imaging and dipole-dipole technique surveys were conducted on the Korope car park inside Osun State University, Osogbo, Southwestern Nigeria. The aim of the study was to use the two equipment to investigate the subsurface rock and to compare the results of using these two resistivity tools in the delineation of the depth to bedrock of the site prior to the concrete flooring. A total of four (4) electrical resistivity field data were collected using the two different resistivity equipment-PASI geophysical machine and the integrated geophysical information system (IGIS) machine.

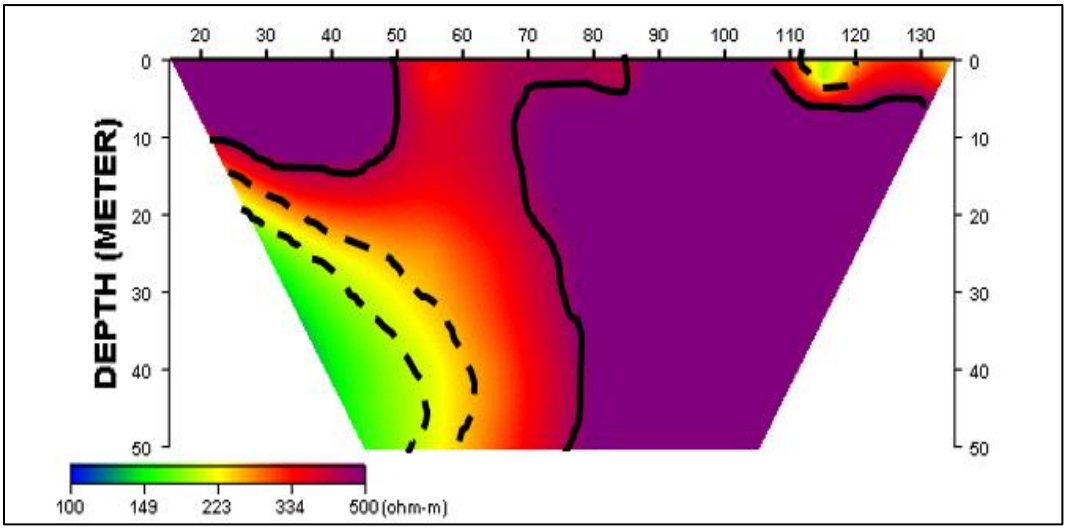

Figure 5: Korope car park 2D-Wenner (IGIS) Pseudo-section

The acquired field data were recorded on the data sheet and later subjected to preliminary interpretation using MS Excel package and then DiprofWin software. The study revealed that the subsurface rock consists of sandy topsoil followed by a lateritic material both of which were underlain by a bedrock. The dipole-dipole interpretation revealed that the subsurface layers of the study area consist of about 10 meters thick weak and incompetent sandy material of resistivity of about 296 Ωm. This layer is underlain by a 4 meters thick low resistance lateritic layer of resistivity value of 372.18 Ωm. The bedrock underlying the sequence is located at a depth of 15 m and has a resistivity of between 4169.09 Ωm, and 4670.132 Ωm. The interpretations obtained using the two pieces of equipment seem to correlate at shallow depth but differ with the results obtained from their Wenner interpretation due to the very high exaggerated values obtained while using IGIS instrument. This makes the inversion of the Wenner result not to correlate effectively.

The result concludes that the depth-to-bedrock interface is best defined using the PASI resistivity instrument compared to the IGIS resistivity meter. Based on the results obtained from the investigations, the following recommendations were made:

(i) For effective delineation of the overburden/bedrock interface, resistivity techniques should be combined and integrated with any other geophysical techniques in order to improve the delineation and accuracy, which includes electromagnetic radar, the potential field method and the shallow seismic refraction method.

(ii) It is also recommended that for any superstructure to be constructed within the study area, the depth of the bedrock must be taken into consideration because it goes a long way towards giving information about the depth to competent layer.

Acknowledgements

This research has received nothing but moral assistance and support from students of the Department of Geological Sciences at Osun State

University, who took an active part in field data acquisition as well as processing. We also want to appreciate the likes of Mr. Alexander Ojo of Alexo Geo-Resources, Akure, Ondo State, for the rental of the PASI resistivity meter and Mr. Salako for the rental of the IGIS resistivity meter. We also wish to extend our appreciation to anonymous reviewers who critically reviewed this paper for their suggested contributions and sincere opinions.

References

Ali, M.A.H.; Mewafy, F.M.;Qian,W.; Alshehri, F.; Ahmed, M.S.;Saleem, H.A. (**2023**) Integration of ElectricalResistivity Tomography and InducedPolarization for Characterization and Mapping of (Pb-Zn-Ag) SulfideDeposits. Minerals, https://doi.org/10.3390/min 13070986

Briggs A Martin., Phillip Goodling, Zachary C. Johnson, Karli M. Rogers, Nathaniel P. Hitt, Jennifer B. Fair and Craig D. Snyder (2022) Bedrock depth influences spatial patterns of summer base flow, temperature and flow disconnection for mountainous headwater streams; *Hydrol. Earth Syst. Sci.*, 26, 3989–4011, 2022; https://doi.org/10.5194/hess-26-3989-2022

David Hart, Steve Mauel, John Luczaj, Esther Stewart (2021): Depth-to-bedrock mapping in Wisconsin; Open-File Report 2021-04 | 2021; Wisconsin Geological and Natural History Survey.

Folahan P. Ibitoye (2023): Geophysical Investigations for Design Parameters Related Geotechnical Engineering; Prototype Engineering Development Institute (National Agency for Science and Engineering Infrastructure), Ilesa, Nigeria, 'DOI: http://dx.doi.intechopen.108712org/10.5772/

Froese D.G, Smith D.G, and Clemet D.T, (2005). Characterizing large river history with shallow geophysics. Geomorphology, 67 (2005), pp. 391-406

HickinA.S, Benjamin Kerr,Barchyn T.E, and Paulen R.C,(2009). Using ground penetrating radar and capacitive coupled resistivity to investigate 3D fluvial architecture and grain size. *Journal of sedimentary research*, 79 (2009), pp. 457-477.

Hirsch M, Laurence R.B, and Peter D.R,(2008). A comparison of electrical resistivity, ground penetrating radar, and seismic refraction result at a river terrace site. *Journal of environmental and engineering geophysics*, 13 (2008), pp. 325-333.

Hsu H.L, Yanites B.J,Chien-chih C, and Yue-Gau C,(2010). Bedrock detection using 2D electrical resistivity imaging. *Geomorphology*, 114 (2010), pp. 406-414

Mochales, T., Casas, A.M., Pueyo, E.L., Pueyo, O., Román, M.T., Pocoví, A., Ansón, D., (2008). predictction of underground cavities by combining gravity, magnetic and ground penetrtrating radar surveys: a case study from the Zaragoza area, NE Spain. Environ.Geol. ,1067–1077.

Najafabadipour A. Kamali G.R. (2017): 3D Modeling and Bedrock Determination Using Electrical Resistivity Inversion; 23rd European Meeting of Environmental

and Engineering Geophysics; DOI: 10.3997/2214-4609.201702108.

Neyamadpour Ahmad, Wan Abdullah, Samsudin, Taib and Behrang Neyamadpour (2010): Comparison of Wenner and dipole–dipole arrays in the study of an underground three-dimensional cavity; Journal of Geophysics and Engineering, Volume 7, Number 1; DOI10.1088/1742-2132/7/1/003.

Panthi, Jeeban and Boving, Thomas B. and Johnson, Carole D. and Pradhanang, Soni Mulmi and Savage, Brian and Ismail, Mamoon (2020): Delineating Bedrock Topography with Geophysical Techniques: An Implication for Groundwater Mapping; http://dx.doi.org/ssrn.4247958.

Revil A, Cary L, Fan Q, Trolard F, and Finzola A, (2005). Self-potential signals associated with preferential ground water flow. *Geophysical Research Letters*, 32 (2005), pp.l07401.

Salami A, Babafemi E. (2020): Delineation of Near-Surface Structural Features Suitable for Groundwater Accommodation Using 1-D and 2-D Resistivity Methods in Igarra, Akoko-Edo, Southwestern Nigeria; Journal of Applied Sciences and Environmental Management; J. Appl. Sci. Environ. Manage. Vol. 24 (7) 1209-1215.

Tye A.M,Williams J.D.O, Trangheim D, Raines M, Keith A, and Holghar K, (2011). Using integrated near-surface geophysical surveys to aid mapping and interpretation of geology in an alluvial landscape. *Near surface geophysics*, 9 (2011), pp. 15-31

Zhou, W., Beck, B.F. and Stephenson, J.B., 2000. Reliability of dipole-dipole electrical resistivity tomography for defining depth-to-bedrock in covered karst terranes. *Environmental Geology*, 39(7), pp.760-766